ACCURATE LOCALIZATION OF CELL NUCLEI IN PAP SMEAR IMAGES USING GRADIENT VECTOR FLOW DEFORMABLE MODELS

Marina E. Plissiti, Christophoros Nikou
Department of Computer Science, University of Ioannina, Ioannina, Greece
marina@cs.uoi.gr, cnikou@cs.uoi.gr

Antonia Charchanti
Department of Anatomy-Histology and Embryology, Medical School, University of Ioannina, Ioannina, Greece
acharcha@cc.uoi.gr

Keywords: Nuclei segmentation, PAP stained cervical smear images, Active contours, Gradient Vector Flow (GVF) snake.

Abstract: In this work, we present an automated method for the detection of cells nuclei boundaries in conventional PAP stained cervical smear images. The proposed method consists of three phases: a) the definition of candidate nuclei centroids set using mathematical morphology, b) the initial approximation of cells nuclei boundaries and c) the application of the Gradient Vector Flow (GVF) snakes for the final estimation of candidate cell nuclei boundaries. It must be noted that the initial approximation of each snake position is obtained automatically, without any observer interference. For the final determination of the nuclei in our images, we perform a fuzzy C-means clustering, using a data set of patterns based on the characteristics of the area enclosed by the final position of the GVF snakes. The proposed method is evaluated using cytological images of conventional PAP smears, which contain 3616 recognized squamous epithelial cells. The results show that the application of the GVF snakes entails in accurate nuclei boundaries, and consequently in the improvement of the performance of the clustering algorithm.

1 INTRODUCTION

The automated segmentation of cell nuclei in PAP smear images is one of the most interesting fields in cytological image analysis. The accurate determination of cell nuclei area in cytological images is important for the correct diagnostic decisions, as the nucleus is the structural part of the cell which exhibits significant changes after the affection of the cell by a disease. However, the visual interpretation of these images is a tedious, time-consuming and in many cases error-prone procedure because of the complexity that these images exhibit. Thus, the high degree of cell overlapping, the lack of homogeneity in image intensity and the variations in dye concentration are challenging issues that an automated segmentation method must overcome.

In the last years, cell nuclei segmentation has been extensively studied by several researchers. A large number of methods applied in many cytological images have been proposed based on morphological watersheds (Lezoray, 2002), (Costa, 1997), fuzzy logic (Begelman, 2004), level sets (Cheng, 2009) and active contours (Bamford, 1998), (Hu, 2004), (Plissiti, 2006), (Plissiti, 2008). Active contours (Kass, 1988), also known as snakes, seem an ideally suited technique for the nucleus segmentation problem. However, snakes require an initial contour estimation close to the real boundary, which is usually obtained manually. This limitation is restrictive for the application of snakes in images such as PAP smear images, where a large number of cell nuclei are depicted in a single image and also significant cell overlapping is observed.

Our work aims at the definition of nuclei boundaries in conventional PAP stained cervical cell images using the Gradient Vector Flow (GVF) snake model (Xu, 1998). The proposed method overcomes the problem of snake initialization because an approximation of nucleus boundary is obtained

automatically for each nucleus in the image. As there could be regions not being cell nuclei, we apply the fuzzy C-means algorithm for the classification of the closed regions (the result of the GVF snakes) in the class of interest (nuclei class) or in the class of undesired findings.

To underpin the accuracy of the GVF snake segmentation, we construct two data sets. The first data set comprises the areas enclosed by the initial position of the snakes and the second data set contains the areas under the final position of each snake. As it is verified by the results, the performance of the method is improved when the data set of the area enclosed by the final snake position are used. This is a confirmation that the obtained contour is an accurate nucleus boundary. The proposed method is fully automated and it can be applied in any microscopic cervical cell sample image.

2 MATERIALS AND METHODS

2.1 Study Group

We have collected 19 images of conventional PAP stained cervical cell slides, which were acquired through a microscope digital camera (Olympus DP71) adapted to an optical microscope (Olympus BX51). We have used a 10× magnification lens and the acquired images were stored in JPEG format. The total number of cell nuclei in the images, which were identified by two expert observers is 3616.

2.2 Segmentation

The purpose of this step is firstly the detection of the location of every nucleus in the images and secondly the determination of the boundary of each nucleus area. This is obtained automatically, as we follow the method proposed in (Plissiti, 2006) and (Plissiti, 2008). This method consists of three individual steps and it is described in the following paragraphs.

2.2.1 Detection of the Candidate Nuclei Centroids

This step is necessary for the determination of the location of every nucleus in each image. It is comprised of two sequential stages: the preprocessing and the determination of the probable location of each nucleus. The outcome of this step is a set of image points which indicate the areas of the image that are occupied by the nuclei of the cells.

In the preprossesing step, the extraction of the background and the definition of smooth regions of interest are achieved. We perform contrast-limited adaptive histogram equalization and global thresholding to the red, green and blue component of the image. In the final binary mask, which is the result of a logical OR operation of these three binary images, all particles with an area smaller than a threshold t are removed, in order to exclude objects that may interfere in the next steps.

The parts of the image found in the preprocessing step contain either isolated cells or cell clusters. Considering that nuclei are darker than the surrounding cytoplasm (Figure 1(a)), we search for intensity valleys in the image. For the formation of homogenous minima valleys we apply the h-minima transform (Soille, 1999) in the red, green and blue components of the original image. The resulted image is used as a mask for the morphological reconstruction of the initial image. In the final image, we search for regional minima and the extracted regions of the image intimate the existence of the cell nuclei (Figure 1(b)). The location of each candidate nucleus is determined with the centroid r_c of each detected intensity valley (Figure 1(c)).

2.2.2 Initial Approximation of the Cell Nuclei Boundaries

After the definition of the locations of each candidate nuclei centroid, we proceed with the initial approximation of the nuclei boundaries, which is a prerequisite for the application of the deformable model. For this purpose we collect some points near the centroid of each nucleus, which are likely lying in the nucleus circumference.

Given the fact that the nucleus is darker than the background, we expect high gradient of the image in each nucleus boundaries. In order to avoid threshold dependent techniques such as edge detectors, we construct an image with each nucleus boundaries pronounced. This image is a result of the subtraction of two images. The first image is the result of the application of an averaging filter in the initial image. The second image is the outcome of successive erosions of the initial image, using a flat disk-shaped structuring element. The result of the subtraction of these two images is an image with all cell nuclei boundaries sharp (Figure 2). In this image, we construct a circular searching grid centered at the

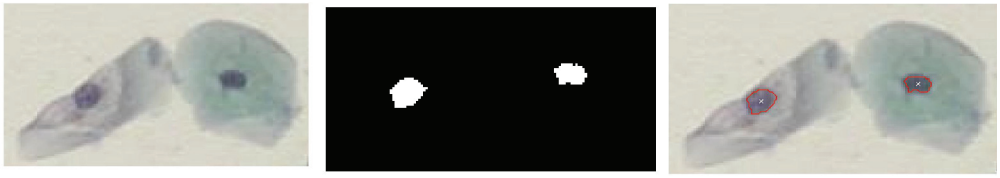

(a) (b) (c)

Figure 1: (a) A part of the initial image containing two cells, (b) the regional minima which correspond to the nuclei and (c) the resulted nuclei centroids.

location of each candidate nucleus centroid. We use 8 radial profiles in equal arc length intervals consisted of 8 points each, and in every radial profile we choose only one pixel (the one with the highest intensity) and we assume that this pixel belongs to the nucleus circumference. In this way, we collect N points for each nucleus boundary and we construct the convex hull using these points. This is used as the initial approximation of the location of the deformable contour.

It must be noted that with the definition of these points in each nucleus circumference, we redefine the nucleus centroid r_c with this formula:

$$r_c = \left(\bar{x}, \bar{y}\right) = \frac{1}{N}\sum_{i=1}^{N}\left(x_i, y_i\right) \tag{1}$$

where x_i, y_i are the coordinates of each circumferential point. After this calculation, we apply a distance dependent rule, in which we eliminate the existence of two or more centroids in an area of a radius that it is smaller than the mean radius of a normal nucleus. The rule is described as follows:

$$\begin{aligned} &\forall\, p=(x,y)\in R_c \\ &if\ exists\ q=\left\{\left(x_q,y_q\right)\middle| D(p,q)\le T\right\} \\ &select\ r=\left\{p,q\,|\,\min\left\{I(p),I(q)\right\}\right\} \end{aligned} \tag{2}$$

where R_c is the set of all centroids, D is the euclidean distance between two points, T is the threshold on the minimum radius and $I(p)$ is the intensity of the image at the point p. With the application of this rule, a significant reduction of the total number of the false positive centroids is achieved.

2.2.3 Application of the GVF Snake

For every nucleus centroid, we apply a deformable model using as initial estimation the convex hull of the circumferential points found in the previous step.

A traditional snake is defined as a curve $\mathbf{x}(s)=\left[x(s),y(s)\right]$, $s\in[0,1]$ and it is deformed under the influence of internal and external (image) forces in order to minimize its energy functional:

$$E = \int_0^1 \left(E_{int}\left(\mathbf{x}(s)\right) + E_{image}\left(\mathbf{x}(s)\right)\right)\ ds \tag{3}$$

As in most conventional snake models, the internal energy is a function of the first and second order derivatives of the curve (for length and curvature minimization), and can be expressed as:

$$E_{int} = \alpha\left|\mathbf{x}'(s)\right|^2 + \beta\left|\mathbf{x}''(s)\right|^2, \tag{4}$$

while E_{image} is defined as:

$$E_{image} = \gamma E_{ext}, \tag{5}$$

where the external energy function E_{ext} takes smaller values at the features of the interest in the image.

A snake that minimizes the energy E must satisfy the Euler equation:

$$\alpha\mathbf{x}''(s) - \beta\mathbf{x}''''(s) - \gamma\nabla E_{ext} = 0. \tag{6}$$

For the solution of this equation, $\mathbf{x}$ is treated as a function of time t as well as s and the partial derivative of $\mathbf{x}$ with respect to t is then set equal to

$$\mathbf{x}_t(s,t) = \alpha\mathbf{x}''(s,t) - \beta\mathbf{x}''''(s,t) - \gamma\nabla E_{ext} \tag{7}$$

The stabilization of the solution $\mathbf{x}(s,t)$ entails in the vanishing of the term $\mathbf{x}_t(s,t)$ and as a result in the solution of (6).

For the external energy, we adopt the approach of the gradient vector flow (GVF) field, as it is described in (Xu, 1998). The GVF field is the vector field $\mathbf{v}(x,y)=\left(u(x,y),\upsilon(x,y)\right)$ that minimizes the energy functional

$$\mathrm{E} = \int\int \mu\left(u_x^2+u_y^2+\upsilon_x^2+\upsilon_y^2\right) + \left|\nabla f\right|^2\left|\mathbf{v}-\nabla f\right|^2 dxdy \tag{8}$$

where $f(x,y)$ is an edge map with larger intensity values near the image edges derived from the initial image $I(x,y)$, ∇f is the gradient of the edge image and μ is a regularization parameter. With this approach the GVF snake is defined as the parametric curve

$$\mathbf{x}_t(s,t) = \alpha \mathbf{x}''(s,t) - \beta \mathbf{x}''''(s,t) + \gamma \mathbf{v} \quad (9)$$

which is solved numerically by discretization in space and time. This deformable model is flexible and it is attracted by the nucleus boundaries. Figure 3 shows the initial estimation and the final contour obtained by the deformation of the model in several examples.

2.3 Clustering of the Candidate Nuclei

The application of the fuzzy C-means classification algorithm (Bezdek, 1992) is necessary for the separation of the segmented regions of the image that belong to the true nuclei and the regions that belong to other regional minima, which do not indicate the existence of a nucleus in the image. For this reason, after the stabilization of each snake in the entire image, a data set of features which are extracted from the area enclosed in the final position of the snake is created. We choose eight features for each candidate nucleus area, which concern the intensity and the shape attributes of the region enclosed by the snake: (i) – (iii) the average intensity of the area in the red, green and blue channel of the image, (iv) the diameter of a circle which has the same area with the region, (v) the proportion of the pixels in the convex hull that are also in the region, (vi) the eccentricity, (vii) the major and (viii) the minor axis length of an ellipse that has the same second moments as the region.

3 EXPERIMENTAL RESULTS

For the evaluation of the method we have to examine the performance of the different steps of the segmentation method, until the application of the fuzzy C- means classification algorithm. The overall loss of the true nuclei in the definition of the candidate nuclei centroids set is 29 nuclei, from which 7 nuclei were missed in the preprocessing step and 22 of them were missed in the detection of regional minima in the image. Thus the total loss of this step is 0.8% and the sensitivity is 99.39%.

In order to evaluate the performance of the segmentation method, the same features are selected for the area of the initial position of the snake. This is a second feature set that is used as input in the fuzzy C-means algorithm, and a comparison of the performance of the method using the first and the second feature set has been done. As it is verified by the results, the use of the feature set obtained from the area enclosed by the final snake position entails in higher classification performance

For the evaluation of the accuracy of the segmentation method, we compare the performance of fuzzy C-means clustering algorithm using the two independent feature sets, the first one obtained from the initial and the second one obtained from the final snake position, as it is described above. The classification performance of the first feature set reaches 82.38% in sensitivity and 75.91% in specificity. On the other hand, the classification performance of the second feature set reaches 91.77% in sensitivity and 74.23% in specificity. As we can see, there is a remarkable improvement in sensitivity, while the specificity is maintained almost in the same levels.

We have also used a variable decision threshold in the fuzzy C- means classification algorithm and we have calculated several values for the sensitivity and the false positive rate, and with these values we have constructed the Receiver Operating Characteristic (ROC) curve for the two different feature sets (Figure 4). As it is observed, the ROC plot of the second feature set is closer to the upper left corner, which means that the overall accuracy of the classification algorithm using the specific feature set is higher than the one using the initial feature set. This implies that the final position of the GVF snake stabilizes in the location of the accurate nuclei boundaries.

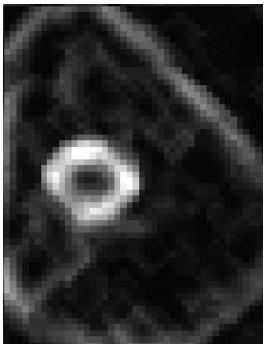

Figure 2: The resulted image of the subtraction of two images (see text for details).

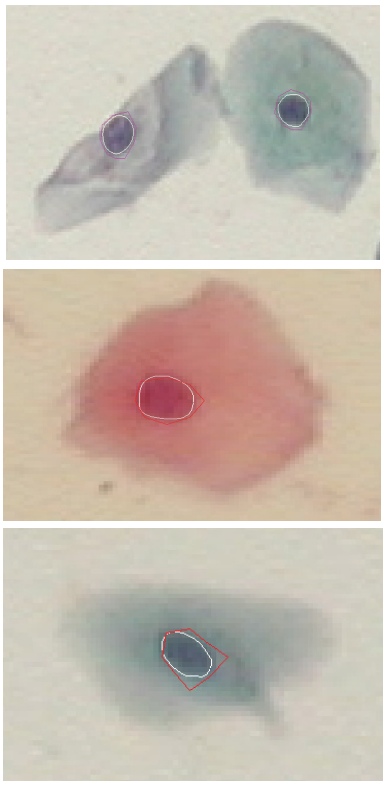

Figure 3: (a)-(c) Examples of the initial estimation of the nuclei boundaries (in red) and the final nuclei boundaries (in white), after the stabilization of the GVF snake.

4 DISCUSSION

The proposed method is applied automatically in conventional PAP stained cervical smear images. For the extraction of acceptable results in all the images of our data set, we have tested several values for the variable parameters of each step of the method. In the preprocessing step, the contrast limited adaptive histogram equalization is performed in image regions of 8×8 pixels and the clip limit is set to 2. For the rejection of objects that are not nuclei we used as a threshold of 500 for the object area, which is sufficient for the elimination of small image artifacts, while preserving the isolated cells in the image. However, the loss of true nuclei in this step is due to the faintly staining of some cells, which makes them undistinguished from the background. As a consequence, the nuclei of these cells are considered as isolated objects in the image background and they are removed.

For the selection of the intensity valleys we choose the threshold value of h=15, which produces the minimum loss of true positives centroids. For the application of the distance dependent rule, for each detected centroid we calculate the minimum euclidean distance from the neighbouring centroids and we used a threshold of 8, which approximates the average nuclei radius, determined after careful examination of the images by an expert cytopathologist.

For the calculation of the gradient vector flow field, we construct an edge map from the initial image, by converting it to a gray scale image and consecutively by applying the Canny edge detector to find the edges. The parameter μ is set to be 0.01. Then, we proceed with the application of the GVF snake with parameters $a = 0.9$, $\beta = 1.5$ and $\gamma = 3$. These values were selected after several experiments in the first image of our dataset and gave acceptable results, as it was verified by an expert cytopathologist. The maximum number of iterations that is allowed for the snake deformations is 20.

5 CONCLUSIONS

We have developed a fully automated method for the segmentation of cell nuclei in PAP smear images. The proposed method overcomes the problem of the detection of the locations of cell nuclei and the restriction of the initial estimation of their boundaries, and it is suitable for the application of the GVF snakes, without any observer interference. As it is verified by the results, the performance of the method is high, as it achieves to determine accurate nuclei boundaries with the stabilization of the active contours. Finally, the proposed method can be used as the basis for further processing of cell images, such as the discrimination of normal and abnormal or malignant cells.

ACKNOWLEDGEMENTS

The authors would like to thank Olga Krikoni for providing the Pap smear slides for the construction of the image data set.

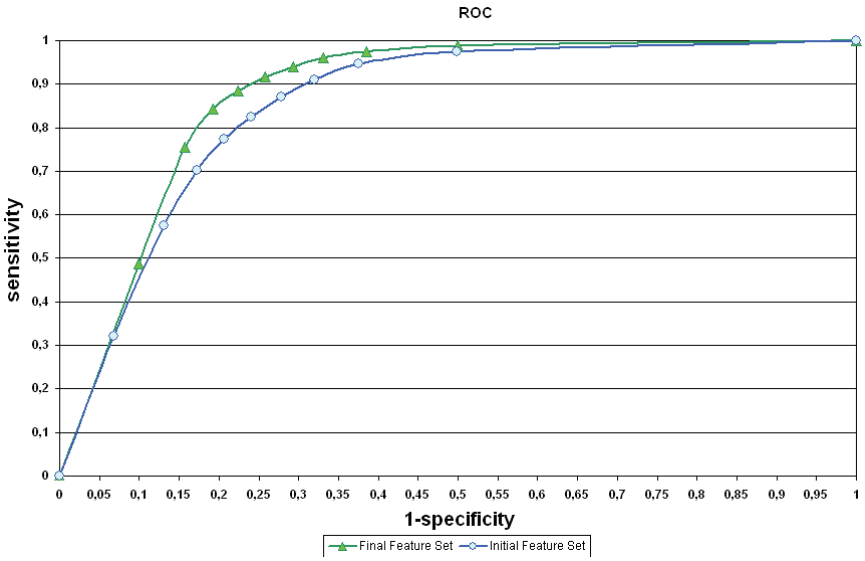

Figure 4: The ROC curve for the initial feature set (blue line) and with the final feature set (green line) for various values of the classification threshold in FCM.

REFERENCES

Lezoray, O., Cardot, H., 2002. Cooperation of color pixel classification schemes and color watershed: A study for microscopic images, IEEE Transactions on Image Processing, Vol. 11, no. 7, pp. 783-789.

Costa, J. A. F., Mascarenhas, N. D. A., De Andrade Netto, M.L, 1997. Cell nuclei segmentation in noisy images using morphological watersheds, Proceedings of SPIE, International Society for Optical Engineering, Vol. 3164, pp. 314-324.

Begelman, G., Gur, E., Rivlin, E., Rudzsky, M., Zalevsky, Z., 2004. Cell nuclei segmentation using fuzzy logic engine, Proceedings of IEEE International Conference on Image Processing (ICIP '04), Vol. 5, pp. 2937-2940.

Cheng, J., Rajapakse, J. C., 2009. Segmentation of clustered nuclei with shape markers and marking function, IEEE Transactions on Biomedical Engineering, Vol. 56, no.3, pp. 741-748.

Bamford, P., Lovell, B., 1998. Unsupervised cell nucleus segmentation with active contours, Signal Processing, Vol. 71, no. 2, pp. 203-213.

Hu, M., Ping, X., Ding, Y., 2004. Applying Fuzzy Growing Snake to Segment Cell Nuclei in Color Biopsy Images, Lecture Notes in Computer Science, Vol. 3314, pp. 672-677.

Plissiti, M. E., Charchanti, A., Krikoni, O., Fotiadis, D. I., 2006. Automated segmentation of cell nuclei in Pap smear images, Proceedings of IEEE International Special Topic Conference on Information Technology in Biomedicine (ITAB '06), Greece.

Plissiti, M. E., Tripoliti,, E. E., Charchanti, A., Krikoni, O., Fotiadis, D. I., 2008. Automated detection of cell nuclei in Pap stained smear images using fuzzy clustering, Proceedings of the 4th European Congress for Medical and Biomedical Engineering (EMBEC '08).

Kass, M., Witkin, A., Terzopoulos, D., 1988. Snakes: active contour models. International Journal of Computer Vision, Vol. 1, pp 321-331.

Xu C., Prince, J., 1998. Snakes, shapes and gradient vector flow. IEEE Transactions on Image Processing, Vol. 7, No 3, pp 359-369.

Soille, P., 1999. Morphological Image Analysis:Principles and Applications, New York: Springer-Verlag.

Bezdek, J. C., Pal, S. K., 1992. Fuzzy Models for Pattern Recognition, New York, IEEE Press.